Kochi Chapter

Indian Geotechnical Conference
IGC 2022
15th – 17th December, 2022, Kochi

Calibrating of rheological parameters and modeling the runout process of debris flows

Minu Treesa Abraham [1][0000-0002-2540-8681] and Neelima Satyam[1] [0000-0002-5434-0671]

[1] Department of Civil Engineering, Indian Institute of Technology Indore, Madhya Pradesh, India - 453552

Abstract. Long runout debris flows are significant geomorphological processes which are crucial in the process of landscape evolution. The flow rheology is very critical in the case of debris flows and most numerical models uses single rheology to understand all debris flows. The existing calibration methods for rheological parameters consider total volume of flow, which is highly challenging when the resolution of topographical data is coarse. In this study, a new numerical model is proposed (Debris Flow Simulation 2D, DFS 2D), which can simulate both debris flows and earth flows, using three rheologies, considering the effect of bed entrainment. DFS 2D provides the output for velocity, height and entrainment at each time step, for each cell. The applicability of the model is tested for a debris flow event happened in China, using Voellmy Salm rheology. The rheological parameters for the event were calibrated using two new approaches proposed in this study. The values of the rheological parameters of the model, dry-Coulomb and turbulent friction, for the event were calibrated, as 0.1 and 1000 m/s^2, respectively. The results indicate that DFS 2D can be satisfactorily used to understand the volume changes and area affected by debris flows.
Keywords: debris flows, numerical modeling, DFS 2D, calibration.

1 Introduction

Debris flows are defined as moving mass of loose particles with high water content, with particle size ranging from clays to rocks, under the influence of gravity. Since this is a mass movement under the influence of gravity, it is considered as a type of landslide. The landslide classification by Varnes [1] uses the word debris to represent material consists of high percentage of coarse particles. Extremely heavy rainfall or snowmelt usually triggers such flows. During precipitation, the flow occurs in two different modes, either triggered by a failure, or due to erosion. The topography of the region decides the flow path, and the flow affects vegetation cover, structures and other materials during propagation. Such flows are principal mode of soil transport in mountainous areas [2]. When the flow happens in human occupied slopes, it has a much higher effect than any other landslide types due to the high velocity. Occurrence of debris flows are very common in Indian hilly terrains including the Himalayas [3–5] and the Western Ghats [6, 7], and hence a rising concern for the authorities.

Identifying the possible runout path of debris flows can help in adopting suitable mitigation measures and other risk reduction strategies. The initial attempts in this regard were the empirical and statistical correlations between the dimensions of landslides, but these cannot provide clarity on the flow dynamics. Numerical models were later adopted to simulate the flows dynamically, with respect to both space and time.

The flow behaviour of most debris flows are non-Newtonian, and the frequently adopted rheologies for modeling are: Coulomb model [8], Bingham model [9] and Voellmy – Salm model [10]. All these models are widely used for back analysis of debris flows, and the choice of model primarily depends upon the material involved in flow, and the terrain conditions. The simplest among these is the Bingham model, due to the assumption of laminar flow with constant values of viscosity and yield strength [11]. This model is suitable for flows with higher fine content. Coulomb-viscous model considers the effect of friction and cohesion unlike the constant yield strength assumption of Bingham model [12]. Voellmy – Salm rheology and its variations are being used to study the effect of both Coulomb friction and turbulence in the flow [7]. This study presents a new numerical model Debris Flow Simulation 2D (DFS 2D) [13], which allows the user to perform the simulation using three different rheologies, to study the flow characteristics. By using three rheologies, the tool allows to simulate different types of debris flows, both in laminar and turbulent conditions. The model also considers the effect of entrainment from the channel bed, which is a key factor determining the final flow volume and its impact on elements along the path. The entrained particles can make abrupt variations in the flow behavior and hence it is a vital aspect to be considered in the numerical modelling [14].

DFS 2D considers the velocity of the flow to be constant along the flow depth, following the shallow water conditions [2]. This makes the analysis simpler, with providing the variation of flow parameters with respect to time, across the considered domain. The governing equations used for analysis are the mass and momentum conservation equations.

2 Methodology

DFS 2D assumes the flow to be single phase, with homogeneous material, based on Savage-Hutter theory [15]. The flow is modelled as a 2-dimensional continuum, using depth integrated shallow water equations. Such an analysis simplifies the three dimensional problem and provides satisfactory details on flow dynamics. The DEM is the primary input which defines the grid space, and the unit dimension in defined by the resolution of the DEM. The model uses 2 dimensional cartesian coordinates x and y in an Euclidian space to define the governing equations [2], given by the following equations:

$$\frac{\partial H}{\partial t} + c_x \frac{\partial (HU_x)}{\partial x} + c_y \frac{\partial \left(HU_y\right)}{\partial y} = Q \tag{1}$$

$$\begin{aligned} \frac{\partial U_x}{\partial t} + c_x U_X \frac{\partial U_x}{\partial x} + c_y U_y \frac{\partial U_x}{\partial y} &= -c_x g \left(S_x + k \frac{\partial (c_x H)}{\partial x} + S_f |U_x| \right) \\ \frac{\partial U_y}{\partial t} + c_x U_y \frac{\partial U_y}{\partial x} + c_y U_x \frac{\partial U_y}{\partial y} &= -c_y g \left(S_y + k \frac{\partial (c_y H)}{\partial y} + S_f |U_y| \right) \end{aligned} \tag{2}$$

where H is the thickness of the flow, and U_x and U_y are the components of velocity in x and y directions respectively. The coefficients c_x and c_y are the cosine values of the angles between horizontal plane and channel bed in the x (α_x) and y (α_y) directions, respectively. The parameter Q is used to incorporates the effect of entrainment and is called the mass source term. Each term in Eq. (2) denotes the accelerations considered.

The term g represents acceleration due to gravity. The convective acceleration is represented in the LHS of Eq 2, which is the time rate of change due to the change in position in space. The RHS considers the time or local acceleration; the first term denotes the acceleration due to gravity, and the second term specifies pressure acceleration within the flow. $S_x = tan\alpha_x$ and $S_y = tan\alpha_y$ are the gradients of slope angles. The term S_f is the gradient of flow resistance, which is determined by the flow rheology. The parameter k is the coefficient of earth pressure (active or passive), and it depends upon the angle of internal friction (φ) of the soil.

The coefficients derived from the velocity values, $|U_x|$ and $|U_y|$ are given by:

$$|U_x| = \frac{-U_x}{\sqrt{{U_x}^2 + {U_y}^2}}$$
$$|U_y| = \frac{-U_y}{\sqrt{{U_x}^2 + {U_y}^2}} \quad (3)$$

where the function of negative sign is to assure that direction of S_f and velocity act in opposite directions.

The effect of rheology is represented by the term S_f in Eq.(2). In DFS 2D, the simplified expression of shear stress was used to derive the value of S_f [16] in Bingham model as :

$$S_f = \frac{1}{\sigma}\left(\frac{3}{2}\tau_C + \frac{3\mu}{H}|U|\right) \quad (4)$$

where σ is the normal stress acting on channel bed, τ_c is the constant yield strength, μ is the viscosity parameter, and $|U| = \sqrt{{U_x}^2 + {U_y}^2}$. For the Coulomb – viscous rheology, the resistance value was followed as:

$$S_f = tan\varphi' + \frac{1}{\sigma}\left(\frac{3}{2}\tau_C + \frac{3\mu}{H}|U|\right) \quad (5)$$

For Voellmy-Salm rheology, S_f is calculated as follows [17]:

$$S_f = \mu_f gH + \frac{g|U|^2}{\xi} \quad (6)$$

where ξ is the coefficient of viscous turbulent friction, and μ_f is the dry-Coulomb friction.

The model is developed in python and an interface was developed using tkinter (Fig. 1). The outputs can be saved in multiple file formats in a destination specified by the user.

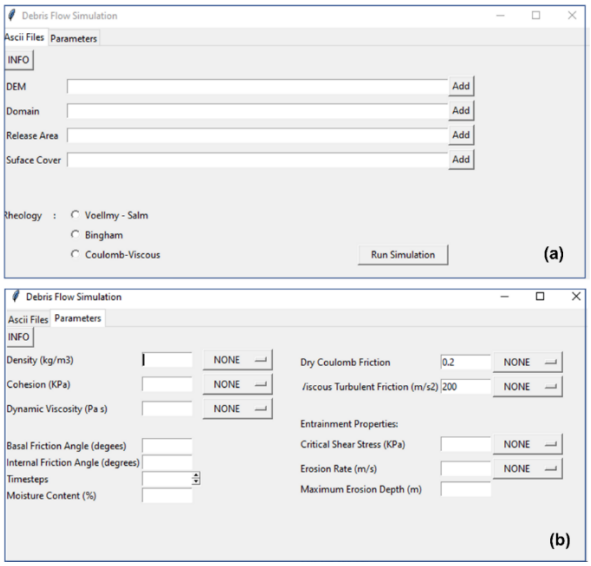

Fig. 1. Interface of DFS 2D. a) rheology AND ascii files b) parametric inputs

The interface has two different tabs. The first tab deals with the rheology and input files while the second tab takes the parametric inputs. An 'INFO' button is added in both the tabs, to provide a brief description about the required inputs. The parametric inputs are again classified into entrainment parameters, soil parameters, and rheological parameters. The soil parameters can be found from laboratory experiments, while the entrainment and rheological parameters cannot be directly obtained. They are usually calibrated using the back analysis of historical debris flows for a particular site.

The outputs are provided in three different formats:

- .txt files for each time step
- .jpg files of heatmaps for each timestep
- .mp4 video showing the changes in each time step

The outputs include the values of flow height, velocity and entrainment, in each cell in each timestep as mentioned above. While the .txt files save the values of flow height, velocity and entrainment for detailed analysis, the mp4 video and heatmaps aid in visualising the flow.

The model was tested for a rainfall induced debris flow event happened in August 2010 in China (Fig. 2). The changes in terrain before and after the event were compared to test the performance of the model. The event was highly turbulent with a significant share of granular materials, and hence Voellmy Salm rheology was selected for the analysis.

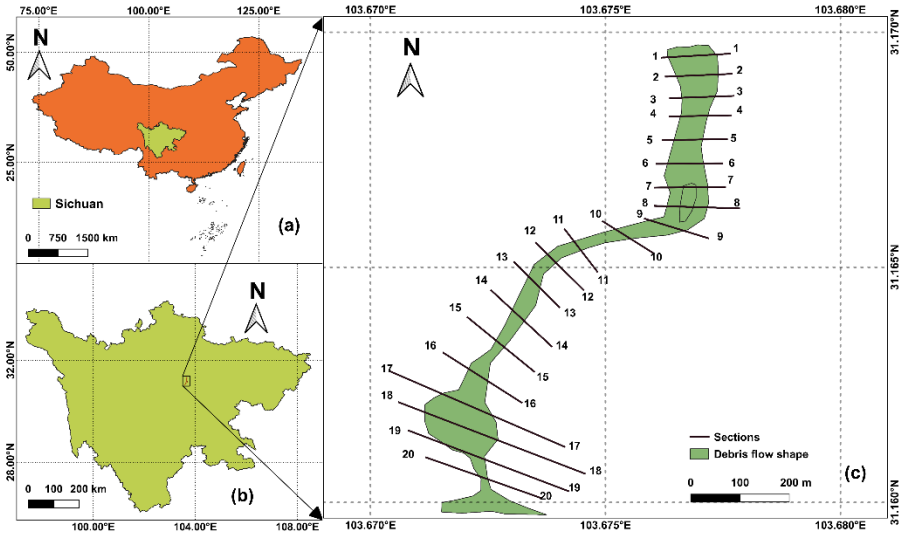

Fig. 2. Location details of study area

The pre and post DEMs of the study area were collected from the Alos Palsar data [18] with a resolution of 12.5 m. For a back analysis, it is important to have the pre and post DEMs from the same source, and Alos Palsar DEM was the finest available source with both the DEMs. The change in terrain conditions after the debris flow were evaluated using the difference between pre and post DEMs, and this data was used for the calibration process. The coarse resolution of DEM is the major challenge in the modeling process. This was overcome by adopting two new strategies for calibration, other than the conventional approach of comparing the modelled flow volume to the observed flow volume. The proposed methods involve a section wise analysis and a cell-by-cell analysis. In the section wise study, multiple cross-sections are considered along the flow path, and the change in cross sectional area due to debris flow of the simulations and the observed data were compared to find the model with least error. The second method involve a cell-by-cell analysis, where the modelled values are compared with the observed values in each grid cell of the DEM. The simulation with the highest agreement with the observed change in terrain is selected as the calibrated one.

3 Results and Discussion

The back analysis explores the applicability of DFS 2D in modelling debris flows. The rheological parameters of the flow need to be calibrated such that the modelled results agree with the observed results. The calibration of friction parameters was carried out by keeping the entrainment parameters constant. For calibration, a trial-and-error approach was adopted by varying the values of both μ_f and ξ. The values of ξ were varied from 100 m/s^2 to 2000 m/s^2 and those of μ_f were varied from 0.01 to 0.40. The upper limit of μ_f was taken as 0.40, considering the higher percentage of granular materials involved in the flow. The resolution of elevation values of the pre and post DEMs was 1 m and hence fine calibration process was not conducted.

For calibration, 20 different sections (Fig. 2) were considered along the runout path. The observed change in cross-sectional area derived from the pre and post DEMs at each section was compared with the modelled change. The maximum flow height simulated at each cell, for different values of μ_f are plotted in Fig. 3.

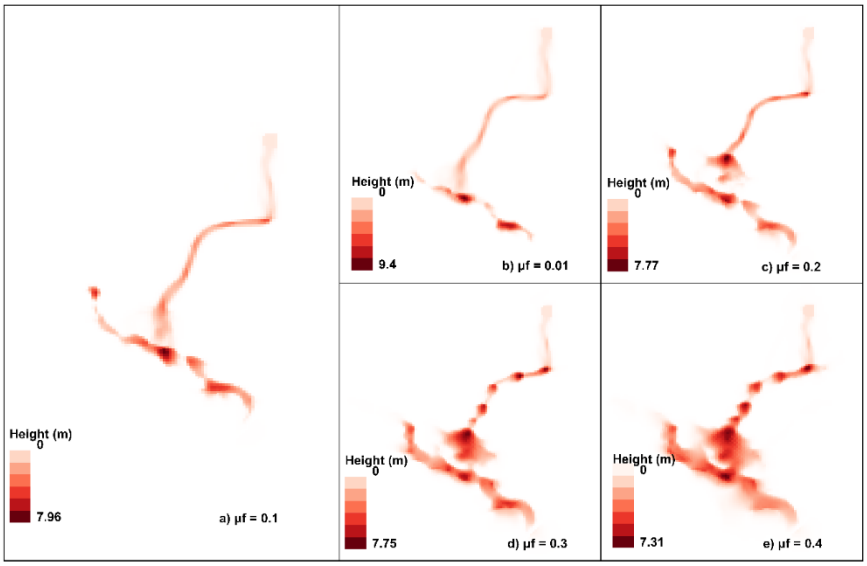

Fig. 3. Effect of μ_f on the debris flow height; ξ = 1000 m/s^2

From Fig. 3, it can be understood that the flow height is amplified at positions where a sudden change elevation or flow direction has occurred. The maximum value of height in all cases were noted at the zone of deposition and the width of flow increased with an increase in μ_f value. The maximum values of flow height increased when the value of μ_f was increased from 0.01 to 0.10 and further increase in μ_f resulted in the decrease of maximum flow height. It was also found that that as the value of μ_f is increased, the number of cells with larger flow height are also increasing. Figure 4 depicts the areas of cross section at different sections, for different values of μ_f.

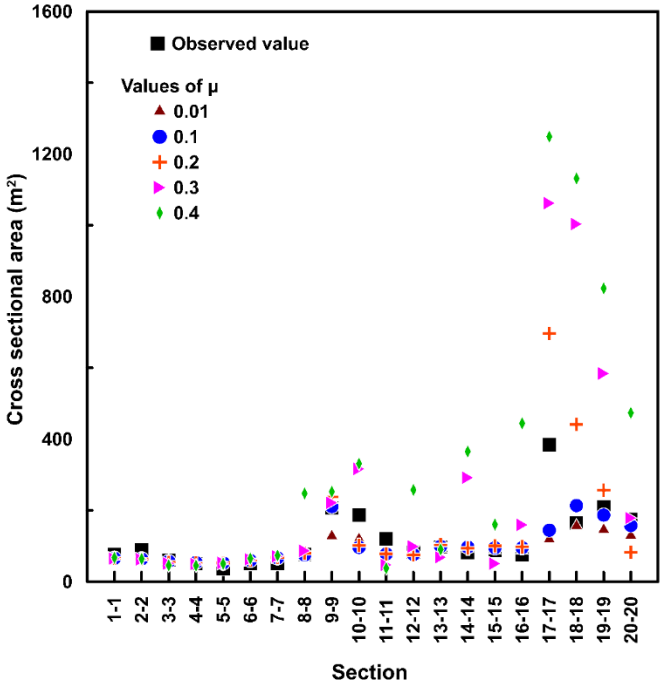

Fig. 4. Scatter plot of observed and modelled areas at different cross sections; ξ = 1000 m/s^2

It can be observed from Fig. 4 that all the trials are in comparable with the observed values upto section 7-7. This is obvious from Fig. 4 as well, as the preliminary cross-sections are having similar areas in all trials. Even though the peak value of flow height is decreased with the rise in value of μ_f beyond 0.10, the larger values of widths led to the over estimation of cross-sectional areas. The trials with μ_f = 0.40 has the maximum area of cross section in all the trials and is largely varying from the observed values. The extreme difference between modelled and observed values is observed at zone of accumulation, where higher values of μ_f overestimates cross-sectional areas. At section 17-17 in the starting of accumulation zone, no simulations are agreeing with the observed values.

From the cross-section-based comparison, it was found that the results were better when μ_f = 0.10, yet all modelled values cannot be assessed this way. To overcome this limitation, the predicted difference in elevation in each grid cell was compared with the observed variation between the pre and post DEMs. The absolute error between the modelled and observed differences in all cells were added up and the model with minimum error can was found. The sum of errors for different values of μ_f are mentioned in Table 1. It can be understood from Table 1 that the sum of errors is minimum when μ_f = 0.10.

Table 1. Sum of absolute errors of all cells for different values of μ_f; ξ = 1000 m/s^2

Dry-Coulomb friction, μ_f	Sum of errors
0.01	744.24
0.10	690.72
0.20	1028.60
0.30	1724.93
0.40	2250.35

Once the value of dry-Coulomb friction has been calibrated, multiple trials were carried out by changing ξ value. The values of peak flow height increased from 10.26 m to 11.26 m when ξ was increased from 100 m/s^2 to 400 m/s^2 (Fig. 5). When the value of ξ was increased beyond 400 m/s^2, the maximum height of flow started decreasing. The difference was insignificant for an increase in ξ from 1000 m/s^2 to 2000 m/s^2. Also, the variation of height of flow in each pixel along the runout path was similar for all trials.

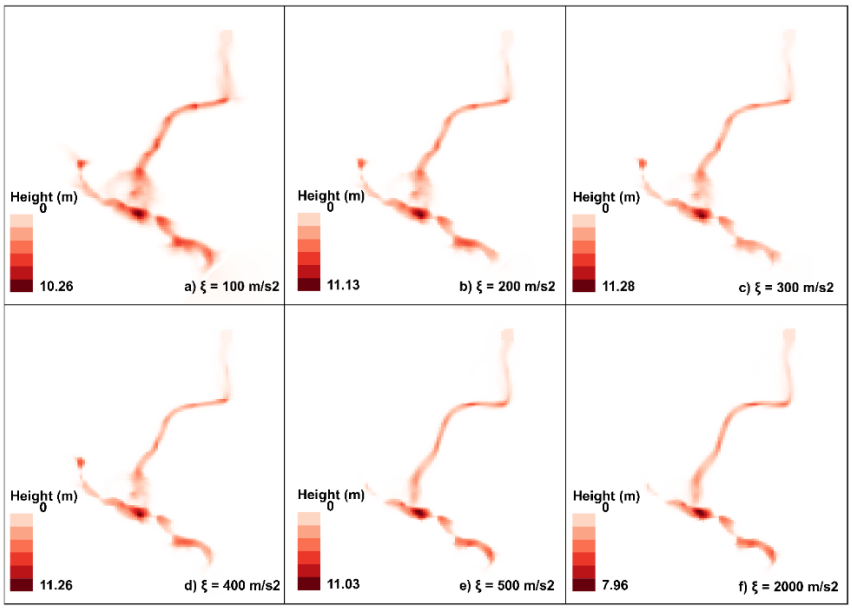

Fig. 5. Effect of ξ on the debris flow height; μ_f = 0.10

To study the effect of ξ in detail, the areas at different cross-sections were compared with the observed values (Fig. 6). Similar to the case of μ_f , the peak variation from observed values were in the zone of accumulation, from section 17-17. The area predicted by the trials with ξ less than 1000 m/s^2 were found to be larger than the observed values and those with ξ = 2000 m/s^2 were smaller than the observed values, in most of the cross-sections.

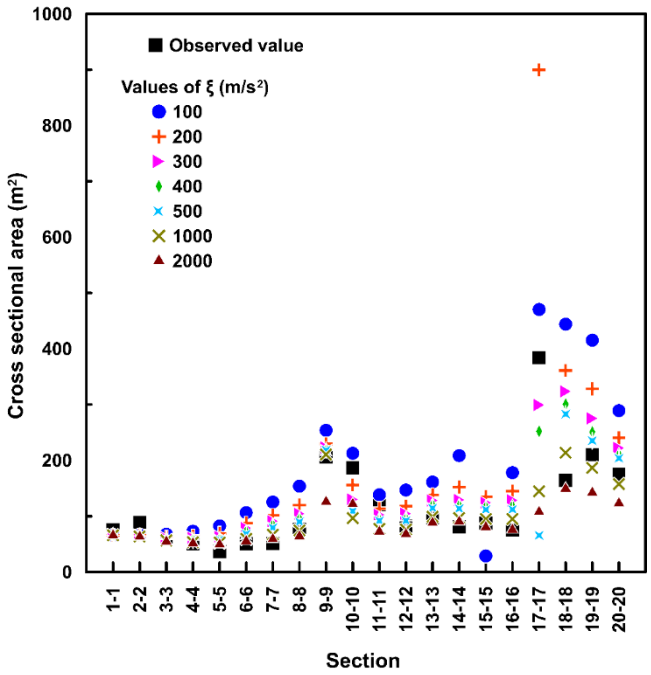

Fig. 6. Scatter plot of observed and modelled areas at different cross sections; μ_f = 0.10

Apart from the cross-section-based study, a cell-by-cell analysis was also conducted for all the trials (Table 2) and it was observed that the results are the best when ξ = 1000 m/s^2. The variations in sum of errors were not as significant as in the case of μ_f. This implies that the flow parameters can be affected more by the variations in μ_f.

Table 2. Sum of absolute errors of all cells for different values of ξ; μ = 0.10

Viscous turbulent friction, ξ (m/s^2)	Sum of errors
100	1329.65
200	1072.50
300	958.80
400	917.21
500	869.82
1000	690.72
2000	740.00

Both the cross-section-based and cell by cell analyses implies that the simulation with μ = 0.10 and ξ = 1000 m/s^2 has the best performance among all the trials. The predicted flow parameters can be assessed in detail to study the runout process.

The rheological parameters for the debris flow considered in this study were calibrated as ξ = 1000 m/s^2 and μ_f = 0.10. The results are in good agreement with the field observations of highly turbulent flow with large sized particles. Since there is no data of the actual flow velocity or the variation of flow parameters with respect to time, only the maximum values are compared with the difference between the pre and post DEMs.

The comparison of areas of cross sections along the flow path shows that the observed and predicted values are in good agreement with each other, except in the case of zone of accumulation. The simulations predict a sudden velocity drop at this section and a slight increase in the area of cross section. It should also be noted that after section 17-17, at the zone of accumulation, the bed erosion is less than that of the predicted value The difference is cross-sectional area is the result of error in predicting the lateral spread of the flow. In the accumulation zone, deposition is more than erosion, however, the mechanism of deposition highly depends upon the water level in the river, which cannot be assessed correctly using the pre and post DEMs alone. Hence the deposition aspect is not discussed in this manuscript.

The flow velocity, height, and depth of entrainment at each cell were calculated by DFS 2D and saved as a text file. When the induced shear stress exceeds the user defined critical shear stress, bed material is entrained from the cell. This has been checked for all cells other than those in the release area. In this analysis, 1.50 kPa was considered as the critical shear stress for entrainment calculations. The bed entrainment values were less in sections with steep slope, even though the velocity values were higher (sections 1-1 to 8-8). When the slopes are less steep and flow occurs with higher velocity, the entrainment values are also higher (Fig. 7). The maximum value of entrainment predicted by the simulation is 7.5 m, which is in good agreement with the observed value of 7 m. The flow started with a release volume of 4790.2 m^3 which got increased to 2,65,342 m^3 at the end of simulation, due to the entrainment. The modelled value is much higher than the value estimated from field observations. This is accounted by the poor resolution of DEM used for the study.

The flow velocity has the maximum value at the middle of cross sections. Towards the edges, the velocity decreases and ultimately the lateral spread of flow is controlled. The general trend of flow height, entrainment and velocity are comparable. At locations closer to crown, value of bed entrainment is higher than the maximum flow height, while it is the reverse at sections beyond 400 m from crown.

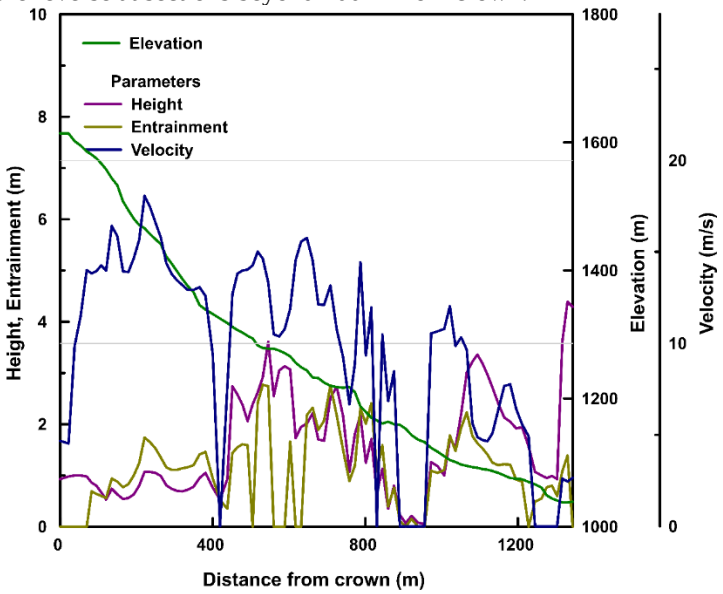

Fig. 7. Peak values of velocity, height, and entrainment recorded along the runout path

Also, the flow began with very high velocity, which got decreased according to the changes in slope. At plane terrains, the entrainment depth and the velocity of flow are decreased. By using DFS 2D, we can calculate the flow height, velocity and bed entrainment of a debris flow at each cell and the results can be used to estimate the impact of flow and energy. The information can be made useful in quantitative risk assessment due to debris flows, and for designing suitable mitigation works.

4 Conclusions

A new debris flow simulation model (DFS 2D), which can consider multiple rheologies and can be used to model flows of varying particle sizes and moisture contents is proposed in this study. DFS 2D also considers the bulking of flow due to bed entrainment, the effect of surface cover and moisture content of the flow. The interactive GUI of DFS 2D lets the user to input the DEM, release area, domain, and surface cover maps in ascii grid format along with the entrainment, soil, and rheological parameters. The model stores the flow height, velocity, and entrainment values in all cells for each time step.

The applicability of DFS 2D was assessed using the data from a major debris flow event happened in China on 13th August 2010. Two different approaches were implemented for calibration, one by considering multiple cross-sectional areas along the flow path, and one by comparing the absolute error of elevation change in each grid cell. The investigation proved that DFS 2D predicted the flow parameters using Voellmy-Salm rheology satisfactorily. The rheological parameters were calibrated as ξ = 1000 m/s^2 and μ_f = 0.10.

The model proves to be a suitable tool to study the runout of debris flows and quantitative risk assessment. It can also be used for calibrating the rheological and entrainment parameters for any region, which can aid in predicting the runout paths of probable failures in the future.

Acknowledgments

The authors would like to acknowledge the financial support from the Department of Space, India, under project number ISRO/RES/4/663/18-19. The authors would also like to thank IMHE, Chengdu for their support in collecting field data.

References

1. Varnes D (1978) Slope Movement Types and Processes. Transp Res Board Spec Rep
2. Beguería S, W. J. Van Asch T, Malet JP, Gröndahl S (2009) A GIS-based numerical model for simulating the kinematics of mud and debris flows over complex terrain. Nat Hazards Earth Syst Sci 9:1897–1909. https://doi.org/10.5194/nhess-9-1897-2009
3. Satyam N, Abraham MT (2022) Forecasting Landslides for Disaster Risk Reduction:

Process-Based Approaches and Real-Time Field Monitoring. In: Kolathayar S, Pal I, Chian SC, Mondal A (eds) Civil Engineering for Disaster Risk Reduction. Springer Tracts in Civil Engineering, Springer, Singapore, pp 147–167

4. Bulzinetti MA, Abraham MT, Satyam N, et al (2021) Combining rainfall thresholds and field monitoring data for development of LEWS . In: EGU General Assembly 2021. Online, p 20172
5. Segoni S, Abraham MT, Satyam N, et al (2021) Application of SIGMA model for landslide forecasting in Darjeeling Himalayas. In: EGU General Assembly 2021. Online, p 669
6. Abraham MT, Satyam N, Jain P, et al (2021) Effect of spatial resolution and data splitting on landslide susceptibility mapping using different machine learning algorithms. Geomatics, Nat Hazards Risk 12:3381–3408. https://doi.org/10.1080/19475705.2021.2011791
7. Abraham MT, Satyam N, Shreyas N, et al (2021) Forecasting landslides using SIGMA model: a case study from Idukki, India. Geomatics, Nat Hazards Risk 12:540–559. https://doi.org/10.1080/19475705.2021.1884610
8. Hungr O, McDougall S (2009) Two numerical models for landslide dynamic analysis. Comput Geosci 35:978–992
9. Malet JP, Laigle D, Remaître A, Maquaire O (2005) Triggering conditions and mobility of debris flows associated to complex earthflows. Geomorphology 66:215–235. https://doi.org/10.1016/j.geomorph.2004.09.014
10. Voellmy A (1955) Ueber die Zerstoerungskraft von Lawinen, Schweiz. Bauzeitung 73:159– 162
11. Coussot P (1994) Steady , laminar , flow of concentrated mud suspensions in open channel. 32:535–559. https://doi.org/10.1080/00221686.1994.9728354
12. Johnson AM, Rodine JR. (1984) Debris flows. In: Brundsenn D, Prior DB (eds) Slope instability. John Wiley, Chichester, pp 257–361
13. Abraham MT, Satyam N, Pradhan B, Tian H (2022) Debris flow simulation 2D (DFS 2D): Numerical modelling of debris flows and calibration of friction parameters. J Rock Mech Geotech Eng. https://doi.org/10.1016/j.jrmge.2022.01.004
14. McDougall S, Hungr O (2005) Dynamic modelling of entrainment in rapid landslides. Can Geotech J 42:1437–1448. https://doi.org/10.1139/t05-064
15. Savage SB, Hutter K (1989) The motion of a finite mass of granular material down a rough incline. J Fluid Mech 199:177–215. https://doi.org/10.1017/S0022112089000340
16. Coussot P (1997) Mudflow Rheology and Dynamics (IAHR Monograph). A.A. Baklema, Rotterdam, Netherlands
17. Christen M, Kowalski J, Bartelt P (2010) RAMMS: Numerical simulation of dense snow avalanches in three-dimensional terrain. Cold Reg Sci Technol 63:1–14. https://doi.org/10.1016/j.coldregions.2010.04.005
18. ASF DAAC (2015) Alaska Satellite Facility Distributed Active Archive Center (ASF DAAC) Dataset: ASF DAAC 2015, ALOS PALSAR_Radiometric_Terrain_Corrected_high_res; Includes Material © JAXA/METI 2007.